Physical and numerical modelling of sand liquefaction in waves interacting with a vertical wall

Hervé Michallet, Emanuele Catalano, Céline Berni, Bruno Chareyre, Valérie Rameliarison, Eric Barthélemy

ICSE6-274

Physical and numerical modelling of sand liquefaction in waves interacting with a vertical wall

Hervé MICHALLET[1], Emanuele CATALANO[2], Céline BERNI[1], Bruno CHAREYRE[2], Valérie RAMELIARISON[1], Eric BARTHELEMY[1]

[1] CNRS/UJF/G-INP, UMR LEGI
BP53 38041 Grenoble cedex 9, France
herve.michallet@legi.grenoble-inp.fr

[2] CNRS/UJF/G-INP, UMR 3S-R
BP53 38041 Grenoble cedex 9, France
catalano@hmg.inpg.fr

Wave induced liquefaction at a coastal structure is studied. Experiments in a glass-wall flume filled with a partially saturated bed of light-weight sediment are presented. Periodic waves and single wave loadings are simulated. For large enough wave conditions an excess pore pressure is recorded within the soil and a liquefaction threshold is reached. Velocity fields obtained from video recordings display large zones of the bed that behave as a fluid. Phases of soil compaction and dilatation are identified. Moreover, a Discrete Element Method – Pore-scale Finite Volume model is used to simulate the wave-sediment interactions. The computation of the coupling between the flow and the motion of the particles enables to reproduce the excess pore pressure that lead to liquefaction and the progressive compaction of the bed.

Key words

Soil fluidization, pore pressure build-up, granular material, hydro-mechanical coupling.

I INTRODUCTION

Wave forcing combined to coastline retreat may weaken or unsettle coastal and port structures. Coupling between dynamic flow and seabed mechanical properties at the vicinity of a structure may trigger scour and liquefaction phenomena leading to easier erosion [de Groot et al., 2006; Sumer et al., 2001]. In field experiments [Mory et al., 2007], liquefaction has been observed at the toe of a vertical wall subjected to intense wave forcing. The phenomenon was identified as momentary liquefaction [Sakai et al., 1992] and promoted by air bubbles trapped inside the bed [Michallet et al., 2009]. The criterion of liquefaction occurrence is estimated as the critical overpressure difference ΔP required to overcome the effective weight of the soil:

$$\Delta P = P_{i+1} - P_i - \rho_w g \Delta z = g \rho' \Delta z (1-n) , \qquad (1)$$

where P_i and P_{i+1} are the pore pressures at two depths in the sand bed, P_{i+1} being Δz below P_i, $\rho' = \rho_s - \rho_w$, with ρ_s and ρ_w the densities of sediment and water, g the gravitational acceleration, and n the porosity. In linear stages, the solid skeleton plays the major role in resisting the wave loadings through the inter-granular contact structures. For strong loadings, wave-induced pore flows can dislocate constituent particles from the skeleton. These particles are thus carried on by the pore fluid resulting in compensated pore pressure build-ups (or excess pore pressure). Also called soil fluidization [e.g. Tzang and Ou, 2006], the threshold (1) is reached as the excess pore pressure approximate the static soil stress, at a given depth below bed surface.

Detailed measurements and visualization of the seabed are not easily obtained in the field. The present study aims at modelling the main physics of the seabed response to wave impact on a coastal structure. To that aim, a physical model using light-weight sediment is devised. Moreover, results from a DEM numerical model are presented and discussed.

II EXPERIMENTS

II.1 Experimental set-up

Experiments are carried out in a 11 m long flume, with glass-wall sides, one extremity consisting of a piston-type wave-maker and the other extremity closed by a Perspex vertical wall. The horizontal bottom is covered with low-density (ρ_s / ρ_w = 1.19) sediment in a 1:20 sloping beach starting at 2 m from the wave-maker (see figure 1). Such a light-weight sediment (median diameter 0.64 mm) has been used by [Grasso et al., 2009] in order to scale wave-induced sediment transport processes by matching Rouse and Shields numbers.

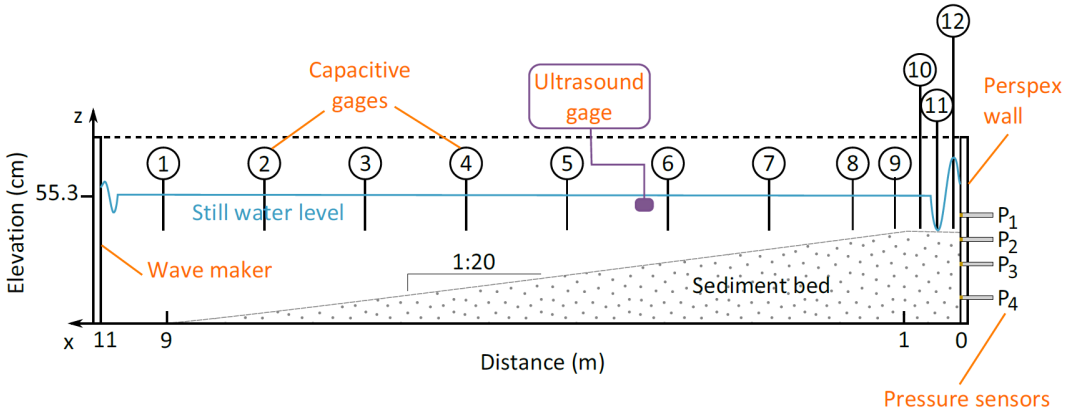

Figure 1: Schematic diagram of the experimental set-up: 12 capacitive gages measure free surface displacements, the ultrasonic gage mounted on a trolley enables bathymetric profiling, the pressure sensors measure inside the pore water in between the sediment grains located against the vertical Perspex wall.

Different techniques for preparing a more compact or loose bed are tested, namely with dry or wet sand in an emptied flume or under water. Somehow simulating the rising tide, filling the flume slowly with water after preparation of the beach allows to trap air bubbles within the bed. (gas content Cg~5 %). Once the bed prepared and the water depth at the desired amount (h_0=55.3\,cm at the wave-maker, 17 cm at the Perspex wall), the initial bed porosity is estimated to range from 0.43 (compact) to 0.52 (loose). The hydraulic conductivity of the bed has been estimated as $k = 3 \times 10^{-3}$ m/s.

Pore pressures are measured at different depths in the soil against the wall (4 cm between sensors), capacitance gauges are used to measure free surface displacements. Furthermore, the different runs are video-recorded, with a focus on the bed region against the wall (25 cm in the x-direction and 12 cm in the vertical z-direction). The video camera has a resolution of 720 × 576 pixels (one pixel thus corresponds to about 0.6 mm), and a sampling of 25 images per second. Displacements fields are computed between two successive images with a Particle Image Velocimetry (PIV) software (Davis) in finding the best correlation over boxes of 16 × 16 pixels. Only motions in the bed are analysed.

II.2 Results

We first present results of a periodic wave interacting with the movable bed (loose condition) at the sea wall. The wave produced by the wave-maker is a linear wave of period 1.5 s and amplitude 4 cm. The first 50 wave cycles are shown in Figure 2. At the wall, the free surface maximum excursion amplifies as a quasi-steady standing wave sets on. The pore pressure within the sand bed is responding periodically with an amplitude of about 500 Pa. The pressure difference between sensors separated vertically by 4 cm is plotted at the bottom of Figure 2. In this dimensionless presentation, the hydrostatic pressure difference corresponds to ΔP=0 and the dimensionless threshold for liquefaction (1) is equal to 0.5 for a porosity taken as 0.5. At each wave crest, a negative peak in ΔP is recorded. In contrast, as the free surface is lowering after the crest, the liquefaction threshold is reached. The pressure difference stays approximately constant until the next rapid rising of the free surface. The process is repeating at each wave cycle, first with increasing peak magnitudes. After about 20 cycles, both negative and positive peaks are decreasing in magnitude.

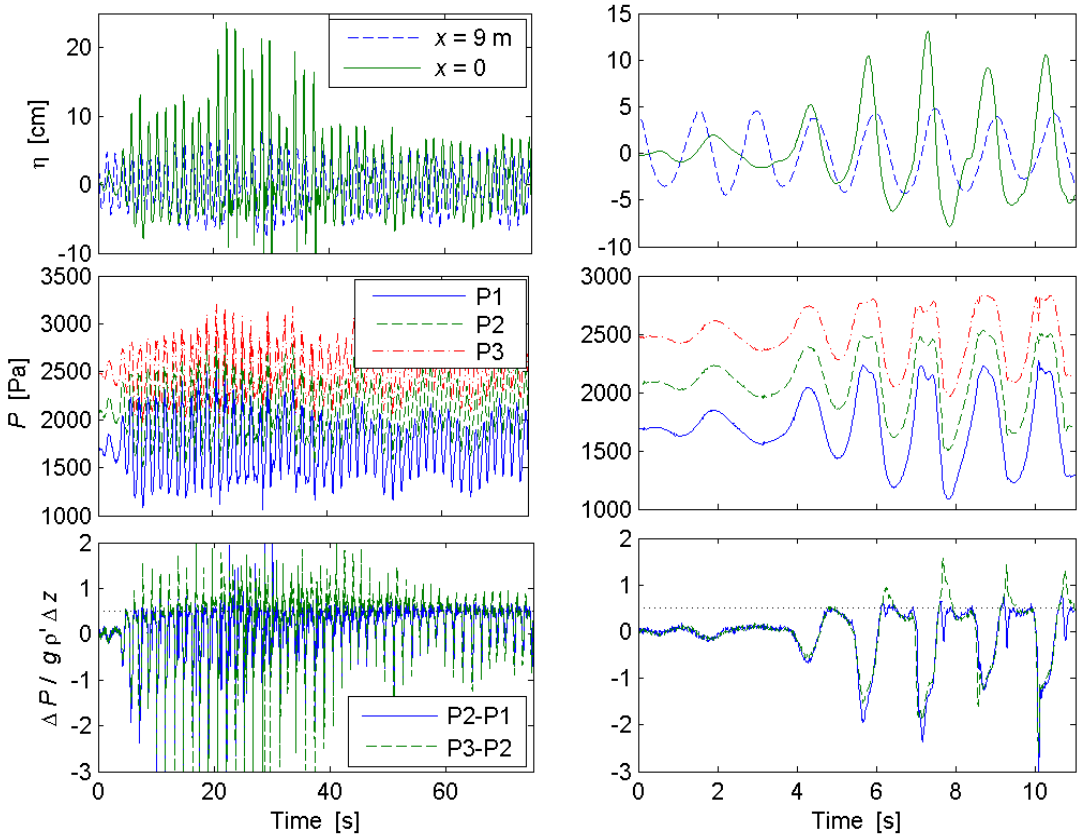

Figure 2: Pressure measurements against the wall, periodic wave condition. Time series of, from top to bottom: free surface elevation (x = 0 is at the wall), pore pressure at z = 0 (bed surface), - 4 and - 8 cm, and dimensionless pressure difference between two sensors. The horizontal dotted line corresponds to the threshold for liquefaction (1) for a porosity n=0.5.

In order to focus on the observation of the soil response to a wave loading, another experiment consisting in producing a single wave train was conducted. The wave-maker motion was a backward then a forward motion (half a sinusoid of 2 s duration) that produces first a lowering of the free surface, then a single wave of about 10 cm height, followed by a second smaller wave. The free surface displacement at 5 m from the wave-maker (x = 6 m from the wall) is shown in Figure 3. The first large wave exactly breaks on the wall at t = 6 s, while the second wave does not break. The pore pressure at the bed surface (sensor P1) and every 4 cm (down to P4 at z = -12 cm) are also shown in Figure 3, as well as the dimensionless pressure difference. The latter clearly indicates that the liquefaction threshold is reached before the wave impact, as the pressure drops with the lowering of the free surface. Large fluctuations are then measured at the wave impact as the pressure becomes a lot larger in the soil upper layer. Just after the wave crest, the pressure difference again corresponds to the liquefied soil value. The same behaviour is observed for the second wave but with a weaker magnitude (for 8 s < t < 9 s). The pressure differences are then slowly decaying toward 0, that corresponds to the sedimentation of the liquefied layers.

Velocity fields of the sediment motion obtained during the first wave impact are shown in Figure 4. Against the wall, velocities are first oriented upwards as the bed liquefies (t = 5.7 s). Strong downwards velocities up to about 10 cm/s are then recorded at the wave crest (t = 6.0 s). After the wave crest, the flow reverses again. The 2D fields of the shear stress modulus, velocity curl and velocity divergence, computed from the horizontal (u) and vertical (v) velocities, are also shown. Large shear stress values are recorded at the wave impact. Cells of strong rotation are identified, indicating soil lenses moving en bloc. The computation of the divergence indicates zones of dilatation (div$\mathbf{U}$ > 0) against the wall as the soil first liquefies and just after the wave crest. Conversely, zones of compaction (div$\mathbf{U}$ < 0) are clearly identified at t = 6 s and t = 7 s.

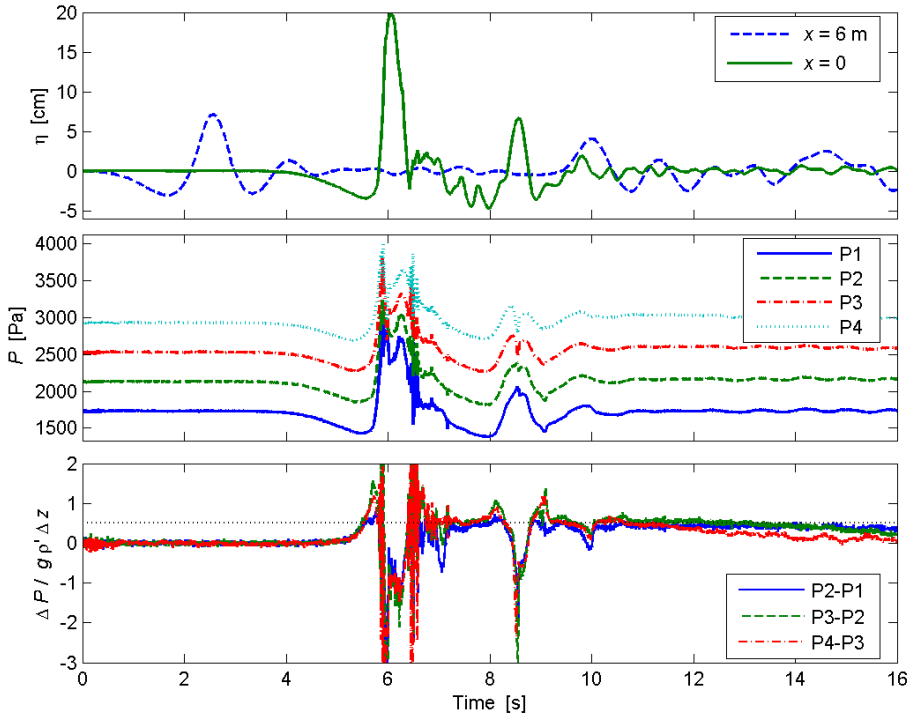

Figure 3: Pressure measurements against the wall, single wave train condition. Time series of, from top to bottom: free surface elevation (x = 0 is at the wall), pore pressure at z = 0 (bed surface), - 4, - 8 cm and – 12 cm, and dimensionless pressure difference between two sensors. The horizontal dotted line corresponds to the threshold for liquefaction (1) for a porosity n=0.5.

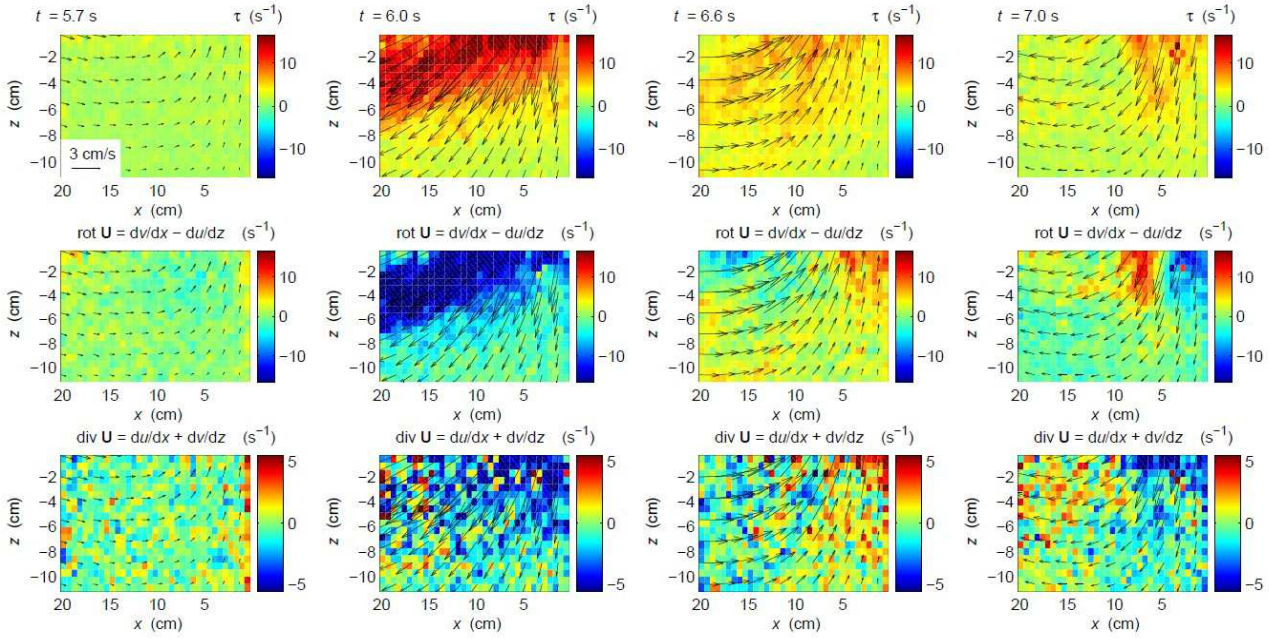

Figure 4: Particle Image Velocity fields of the sand grains motion at 4 instants of the wave impact on the wall shown in Figure 3, superimposed on the shear stress modulus (top), curl (middle) and divergence (bottom). The wall is at x = 0, the bed level at z = 0.

III NUMERICAL MODELLING

III.1 Hydro-mechanical modelling using DEM – PFV coupling

The development of numerical simulations for such complex couplings is a challenging problem. The changes in the state of the seabed sediment are such that it may be described alternatively as a loose granular material in the sense of soil mechanics or as a dense suspension in the sense of fluid dynamics. Clearly, classical constitutive laws fail to cover such a range of mechanical behaviour. Well suited for such situation are discrete granular models based on explicit dynamics, as in the "discrete element method" (DEM). Coupling DEM with fluids is another challenging problem however, since the numerical solution of the Stokes equations is a computationally demanding task, especially for complex three-dimensional pore geometries. A new method for simulating internal flow in granular materials have been developed recently [Chareyre et al., 2011]. In this method, the flow problem is solved using a finite volume scheme, effectively upscaling Stokes equations at the level of pores of the materials. The method is referred to as "Pore scale Finite Volumes" (PFV). It is implemented and coupled with a DEM model of granular material in the open-source DEM software *Yade-DEM* [Šmilauer et al. 2010]. Recent results obtained with this method are reported in the next section.

III.2 Results

In the simulation, a domain of length L = 2 m, 0.8 m high and 0.7 m wide, is filled with 5,000 particles of average diameter d = 0.061 m (0.055 m < d < 0.067 m) and density ρ_s = 2,600 kg/m^3 (see Figure 5). The simulation are performed assuming that the soil is saturated by an incompressible viscous fluid. The pore fluid has the density of water (ρ_w = 1,000 kg/m^3) but a large viscosity (μ = 100 Pa s) in order to compensate for the large size of the particles (the corresponding free fall settling velocity is about 3 cm/s). The initial arrangement of the particles corresponds to a relatively loose soil with porosity n = 0.435. The hydraulic conductivity is $k = 10^{-3}$ m/s. A cycling pressure is imposed at the upper boundary of the domain, that reads:

$$P = P_0 \sin\left(\frac{2\pi t}{T}\right)\cos\left(\frac{\pi x}{L}\right), \tag{2}$$

with P_0 = 1,000 Pa, thus simulating a standing wave of period T = 0.5 s and amplitude 10 cm with a node at x = 1 m and two anti-nodes at x = 0 and x = 2 m. Virtual pressure sensors are placed in the domain with a spacing Δz = 12 cm. A characteristic time of consolidation, of the liquefied layer of particles between two sensors, can be computed as:

$$\tau = \frac{\Delta z}{k}\frac{\rho_w}{\rho_s - \rho_w}. \tag{3}$$

The parameters chosen in the model leads to a value of τ = 75 s which is similar to that which can be computed from the values of the parameters in the physical model.

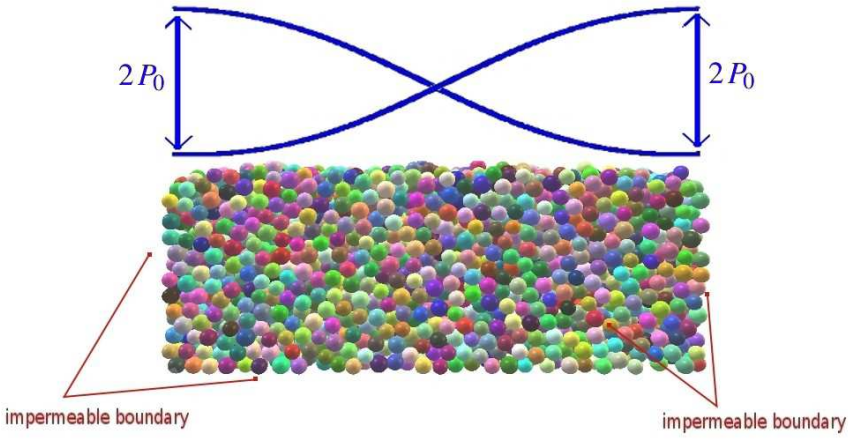

Figure 5: Diagram of the computational domain and forcing.

The pore pressures computed at 6 elevations along the wall are plotted in Figure 6. The pressure is rapidly increasing during the first cycle so that the dimensionless pressure difference is reaching the liquefaction threshold. This pressure increase can be seen as the weight of a (1 - n) packing soil of particles loosing contact. Along with cycles repeating, positive and negative peaks in the pressure difference tend to increase in magnitude and look very similar to the ones measured in the experiments (shown in Figure 2).

The computed pressures at the node of the standing wave are shown in Figure 7. At this location, the oscillatory component of period 0.5 s is very weak. A pore pressure regular increase during the first cycle is clearly seen. The liquefaction first occurs in the upper part of the domain. The dimensionless pressure difference is starting to decrease after about 10 cycles in the lower part of the domain. This is corresponding to a re-arrangement of the particles and consequently a compaction of the soil.

The evolution over the first 50 cycles of the average porosity in the domain is plotted in Figure 8. It clearly shows that the bed is compacting in the process.

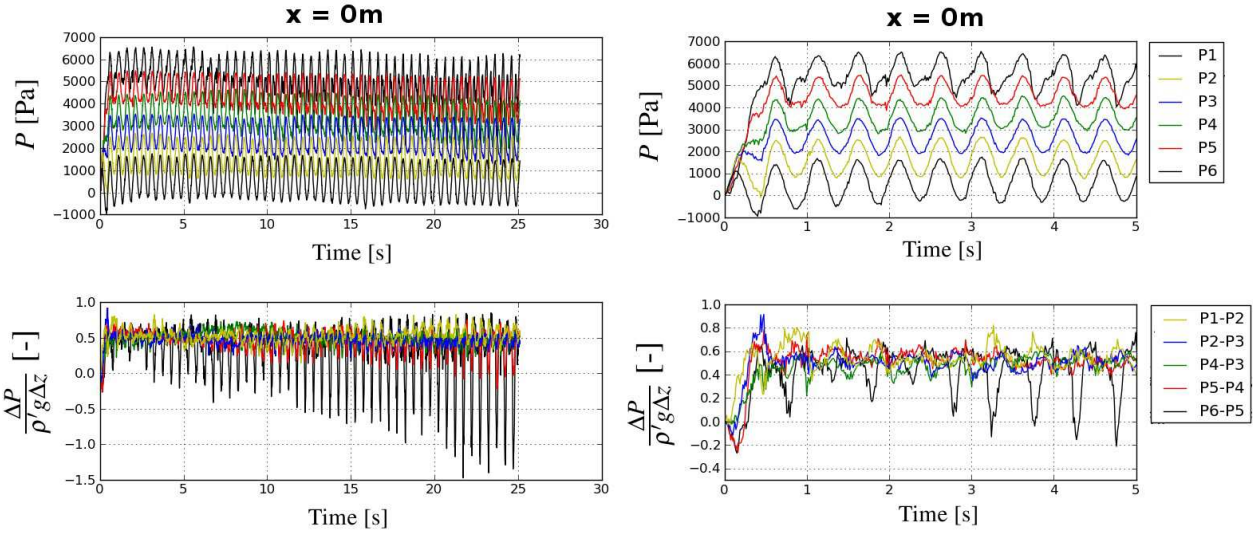

Figure 6: Computed pressure against the wall. Time series of (top) pore pressure at z = - 2.7cm (P6), and every 12.24 cm down to - 63.9 cm (P1), and (bottom) dimensionless pressure difference between two virtual sensors.

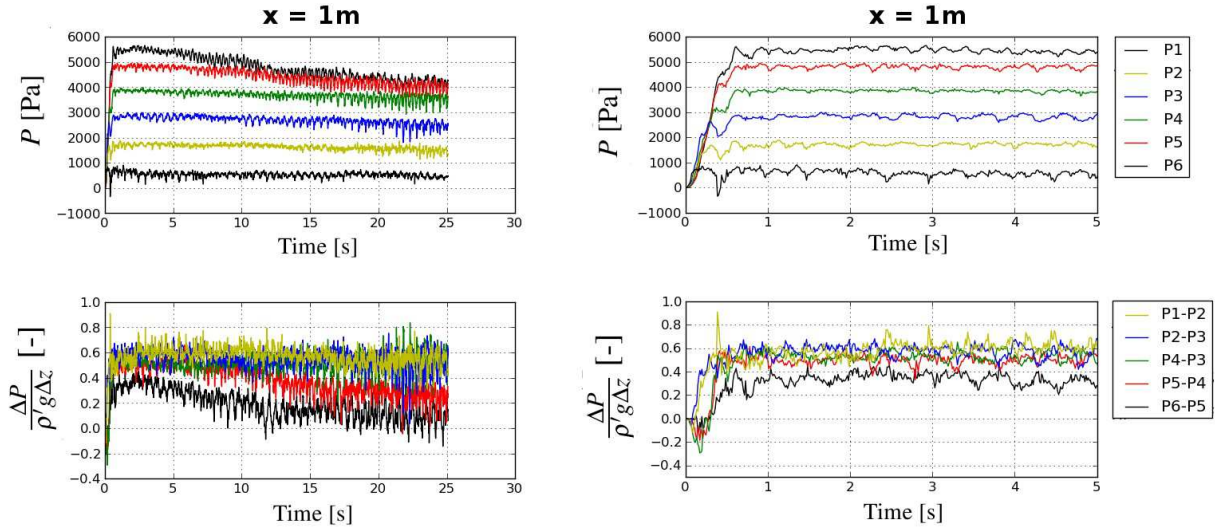

Figure 7: Computed pressure 1 m off the wall. Time series of (top) pore pressure at z=-2.7cm, and every 12.2 cm down to -63.9 cm, and (bottom) dimensionless pressure difference between two sensors.

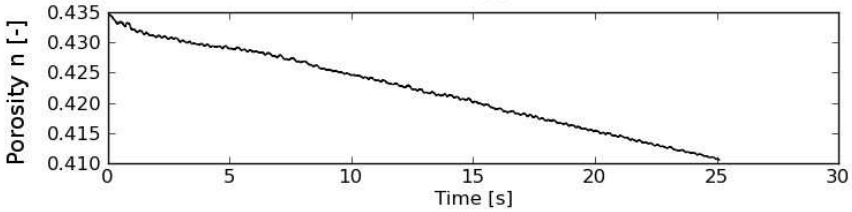

Figure 8: Computed average porosity evolution with time.

IV CONCLUSIONS

A physical model for studying liquefaction occurrence in the wave loading against a vertical wall was described. For large enough wave conditions, and for a loose and partially-saturated bed, an excess pore pressure is recorded within the soil and a liquefaction threshold is reached. A large zone of the bed then clearly behaves as a fluid. Sand grains displacements were quantified. Phases of soil compaction and dilatation were identified. As runs are repeated, the bed becomes more compact and well-saturated and the liquefaction phenomenon tends to vanish.

In the periodic wave tests, the solicitation period being small in front of the consolidation time ($T \ll \tau$), liquefaction was obtained by pore pressure build-up, as described by [Sumer et al., 1999; Tzang and Ou, 2006] for instance. On the other hand, a single loading can lead to momentary liquefaction of the partially saturated bed, as observed previously in the field by [Mory et al., 2007].

Besides, liquefaction by pore pressure build-up was reproduced numerically. It is found that the governing mechanisms of wave-sediment interactions can be reproduced by a coupled DEM – Pore-scale Finite Volume model. Current research work aims at improving the predictive power of this model and conducting more detailed comparisons with the experiments.

V ACKNOWLEGMENTS

The technical support of J.-M. Barnoud, M. Bergonzoli, L. Vignal, M. Lagauzère and F. Bonnel is gratefully acknowledged. J. Chauchat provided very useful comments on the computation of the shear stress modulus and estimation of the hindered settling. This work is funded by project Hydro-Fond: “Réalisé avec le soutien du ministère de l'écologie, du développement durable, des transports et du logement, direction générale des infrastructures, des transports, et de la mer, dans le cadre du programme C2D2 du RGCU”. The power supply provided by G-INP during the experiments was also greatly appreciated.

VI REFERENCES

Chareyre B., Cortis A., Catalano E., Barthélemy E. (2011). Pore-scale modeling of viscous flow and induced forces in dense sphere packings. *Transport in Porous Media*, doi: 10.1007/s11242-011-9915-6.

de Groot M.B., Bolton M.D., Foray P., Meijers P., Palmer A.C., Sawicki A., Teh T.C. (2006). – Physics of liquefaction phenomena around marine structures. *ASCE J. Waterw. Port Coastal Ocean Eng.* 132(4):227-243.

Grasso F., H. Michallet, E. Barthélemy, R. Certain (2009). Physical modeling of intermediate cross-shore beach morphology: Transients and equilibrium states. *J. Geophys. Res*. 114:C09001.

Mory M., Michallet H., Bonjean D., Piedra-Cueva I., Barnoud J.-M., Foray P., Abadie S., Breul P. (2007). A field study of momentary liquefaction caused by waves around a coastal structure. *ASCE J. Waterw. Port Coastal Ocean Eng.* 133(1):28-38.

Michallet H., Mory M., Piedra-Cueva I. (2009), Wave-induced pore pressure measurements near a coastal structure, *J. Geophys. Res.*, 114: C06019, doi:10.1029/2008JC005071.

Sakai T., Hatanaka K., Mase H. (1992). Wave-induced effective stress in seabed and its momentary liquefaction. *ASCE J. Waterw. Port Coast. Ocean Eng.,* 118(2):202–206.

Šmilauer V., E. Catalano, B. Chareyre, S. Dorofeenko, J. Duriez, A. Gladky, J. Kozicki, C. Modenese, L. Scholtès, L. Sibille, J. Stránský, K. Thoeni (2010). Yade Reference Documentation. *In Yade Documentation* (V. Šmilauer, ed.), http://yade-dem.org/doc/

Sumer B.M., Fredsøe J., Christensen S., Lind M.T. (1999). Sinking/floatation of pipelines and other objects in liquefied soil under waves. Coast. Eng. 38: 53–90.

Sumer B.M., R.J.S. Whitehouse, A. Torum (2001). Scour around coastal structures: A summary of recent research. *Coastal Eng.* 44:153-190.

Tzang S.-Y., Ou S.-H. (2006). Laboratory flume studies on monochromatic wave-fine sandy bed interactions. Part 1. Soil fluidization. *Coastal Eng.* 53:965-982.